Quantification of Sauter Mean Diameter in Diesel Sprays using Scattering-Absorption Extinction Measurements

Gabrielle L. Martinez*, Gina M. Magnotti, Benjamin W. Knox, and Caroline L. Genzale
Woodruff School of Mechanical Engineering
Georgia Institute of Technology
Atlanta, GA 30332 USA

Katarzyna E. Matusik, Daniel J. Duke, Christopher F. Powell, Alan L. Kastengren
Argonne National Laboratory
Argonne, IL 60439 USA

Abstract

Quantitative measurements of the primary breakup process in diesel sprays are lacking due to a range of experimental and diagnostic challenges, including: high droplet number density environments, very small characteristic drop size scales (~1-10 μm), and high characteristic velocities in the primary breakup region (~600 m/s). Due to these challenges, existing measurement techniques have failed to resolve a sufficient range of the temporal and spatial scales involved and much remains unknown about the primary atomization process in practical diesel sprays. To gain a better insight into this process, we have developed a joint visible and x-ray extinction measurement technique to quantify axial and radial distributions of the path-integrated Sauter Mean Diameter (SMD) and Liquid Volume Fraction (LVF) for diesel-like sprays. This technique enables measurement of the SMD in regions of moderate droplet number density, enabling construction of the temporal history of drop size development within practical diesel sprays. The experimental campaign was conducted jointly at the Georgia Institute of Technology and Argonne National Laboratory using the Engine Combustion Network "Spray D" injector. X-ray radiography liquid absorption measurements, conducted at the Advanced Photon Source at Argonne, quantify the liquid-fuel mass and volume distribution in the spray. Diffused back-illumination liquid scattering measurements were conducted at Georgia Tech to quantify the optical thickness throughout the spray. By application of Mie-scatter equations, the ratio of the absorption and scattering extinction measurements is demonstrated to yield solutions for the SMD. This work introduces the newly developed scattering-absorption measurement technique and highlights the important considerations that must be taken into account when jointly processing these measurements to extract the SMD. These considerations include co-alignment of measurements taken at different institutions, identification of viable regions where the measurement ratio can be accurately interpreted, and uncertainty analysis in the measurement ratio and resulting SMD. Because the measurement technique provides the spatial history of the SMD development, it is expected to be especially informative to the diesel spray modeling community. Results from this work will aid in understanding the effect of ambient densities and injection pressures on primary breakup and help assess the appropriateness of spray submodels for engine computational fluid dynamics codes.

*Corresponding author: gmartinez36@gatech.edu

Introduction

In direct injection engines, spray breakup processes are known to affect engine-out emissions and efficiency [1, 2, 3, 4]. Thus, developing cleaner and more fuel-efficient engines require a fundamental understanding of the physical mechanisms governing spray breakup. However, spray atomization is not well understood due to the challenges of directly observing this process and simultaneously resolving the large span of characteristic length and time scales (O[μm] and O[ns], respectively) [1].

To improve understanding of the spray breakup process and guide the development of predictive computational design tools, quantitative spray measurements are needed. Under non-vaporizing conditions, droplet sizing measurements can be used to assess theoretical spray breakup predictions. Although Phase-Doppler Anemometry (PDA) measurements can provide point-wise statistics of droplet size and velocity [5, 6, 7], sampling requirements make such measurements challenging in dense sprays [7]. To quantify the resultant droplet size distribution in diesel sprays, alternative diagnostics to conventional droplet sizing techniques must be employed.

Argonne National Laboratory has developed a droplet sizing technique which utilizes x-ray radiography measurements, an absorption based measurement technique, which quantifies the projected density distribution in dense regions of sprays [8, 9]. Although x-ray radiography cannot directly quantify droplet sizes, advances at the x-ray beamline have utilized x-ray radiography measurements to quantify droplet sizes using the ultra-small angle x-ray scattering (USAXS) measurement technique [10, 11]. Although this technique is beneficial to characterize spray breakup, it is very time and resource intensive. Relying on USAXS to fully characterize spray breakup would take years to understand the complicated physics involved in the spray breakup process. Another experimental technique that is less time and resource intensive is needed to accelerate our understanding of spray breakup [11, 12, 13, 14].

A new collaborative experimental campaign between the Georgia Institute of Technology (Georgia Tech) and Argonne National Laboratory has recently been developed that combines existing x-ray and visible-light extinction measurement techniques from each institution, yielding quantitative droplet sizes in diesel-like sprays at engine-relevant ambient and injection pressures. The visible-light scattering measurements are jointly proportional to liquid volume fraction (LVF) and mean droplet size, while the x-ray absorption measurements are logarithmically proportional to liquid mass, or volume fraction under isothermal conditions. Thus, the ratio of path-integrated x-ray and visible light extinction measurements quantify the path-integrated Sauter mean diameter (SMD) [13]. Visible-light scattering measurements at Georgia Tech were performed using diffuse back illumination (DBI), whereas Argonne utilized x-ray radiography to measure the x-ray absorption. In this work, we introduce the experimental setups and theory for each of these measurements and demonstrate the methodology developed to extract the SMD from the joint measurements. We further discuss important considerations for processing these measurements, including uncertainties in the co-alignment of measurements taken at different institutions and careful identification of viable regions where the measurement ratio can be accurately interpreted. Based on this analysis, we provide estimates on the uncertainty of the measurement and the resulting SMD.

Visible-Light Scattering Extinction Measurements

At Georgia Tech, the visible-light scattering extinction experiments were performed in a continuous-flow optically-accessible high-temperature, high-pressure spray chamber [15]. This spray chamber can create engine-relevant quasi-static ambient environments with air, N_2, or any mixture of the two, at a maximum temperature and pressure of 950 K and 100 bar, respectively. All the experiments for this study were conducted with air at room temperature and 1 bar backpressure. There exists approximately 100 mm of optical access at the front, sides, and the top of the chamber. The spray chamber was designed by Advanced Combustion Gmbh and is like other continuous flow-through spray chambers in the literature [16]. The injector used for the experiments was a solenoid diesel injection nozzle, Spray D #209133, provided by the Engine Combustion Network (ECN) [17]. The nozzle features a single, axially-drilled, tapered orifice (measured k-factor of K = 0.8) with a exit diameter of 186 μm [18, 19]. A Bosch diesel common-rail and air-actuated piston pump (MaxPro) delivered liquid fuel to the injector at 50 MPa.

Line-of-sight, 2-D scattering maps of the spray were developed by utilizing a Diffused Back-Illumination (DBI) imaging technique following the recommendations of Westlye et al. [20], as shown in figure 1. The spray was illuminated using a Light-Speed Technologies high-power white LED, with a pulse width

of 90 ns. A Photron SA-X2 high-speed camera, fitted with a 50 mm f/1.2 lens, captured the spray at 72 kfps, while the LED pulsed every other frame at a rate of 36 kfps. The camera captured a dark frame every other frame, which allowed the sensor to reset prior to the next frame. Westlye recommends this procedure to reduce error in the measured extinction due to ghosting, which is residual charge still left on the sensor for the next frame. The image resolution for this arrangement was approximately 77.7 μm/pixel.

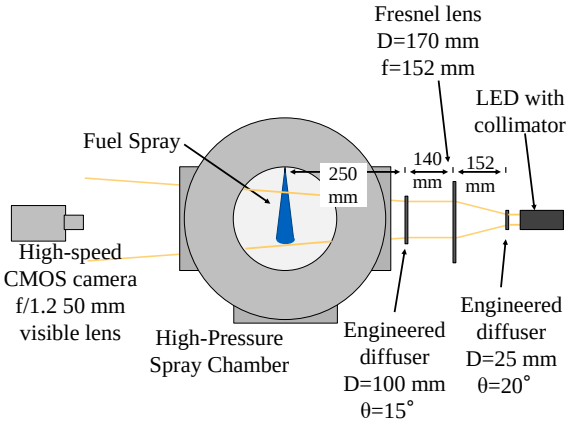

Figure 1. Experimental arrangement for Diffuse Back Illumination (DBI) high-speed imaging of diesel spray, showing the LED with collimator, Fresnel lens, engineered diffusers, spray chamber and the high-speed camera.

The measured outcome of this experimental technique is the optical thickness. This metric is quantified by measuring the intensity of the illumination beam before and after it intercepts the spray. The LED illuminates the chamber before the fuel injection starts and provides a 2-D measurement of the incident light intensity. Once the injection begins, the high-speed camera records the attenuated light after it has passed through the chamber and interacted with the spray. The incident and attenuated light intensity, I and I_o, respectively, are related to the optical thickness, τ, using the Beer-Lambert law,

$$\frac{I}{I_o} = e^{-\tau} \qquad (1)$$

Using the Mie solution to Maxwell's equation, which provides an analytical solution for the 3-D scattering and absorption behavior for a light wave interacting with a spherical object [21], the optical thickness, τ, can be related to the characteristics of the droplet field, including droplet size, d, and liquid volume fraction, LVF [13],

$$\tau = \alpha_{ext} z = \frac{\overline{C_{ext}}}{\overline{\pi d^3/6}} \cdot LVF \cdot z \qquad (2)$$

where, $\overline{C_{ext}}$, is the droplet number-weighted mean extinction cross section, and $\overline{\pi d^3/6}$ is the number-weighted mean droplet volume, within the probed measurement volume of path-length z. Because analytical interpretation of Beer-Lambert's law can only be applied in regions of single scattering, the DBI technique is limited to the periphery of the spray where $\tau \leq 2$. A conservative estimate of the optical thickness limit where multiple scattering errors occur is $\tau > 1$, but errors due to multiple scattering are low for moderate optical thickness levels ($1 < \tau < 2$) when the measurement involves small collection angles and small droplets [22, 23], which are expected conditions for our measurements.

To obtain a two-dimensional distribution of τ from the DBI measurement technique, the attenuated light intensity, I, is time-averaged throughout the steady portion of injection. Ten injection events are then ensemble-averaged to yield the 2-D optical thickness map shown in Figure 2. The condition of interest in this work is for the ECN Spray D injector at an ambient density of 1.2 kg/m^3 and an injection pressure of 50 MPa.

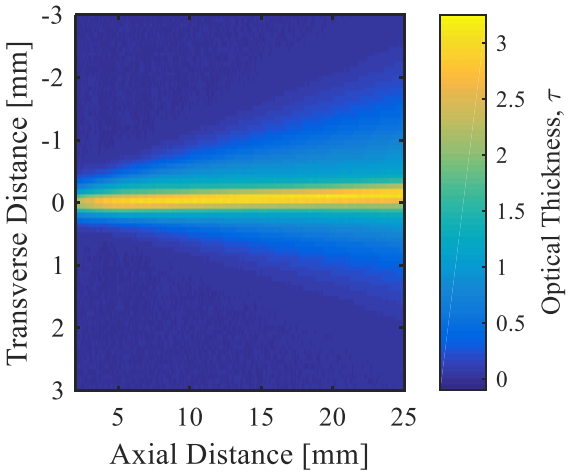

Figure 2. Example 2-D optical thickness map from DBI measurements for Spray D. Experimental condtions: P_{amb} = 1.2 kg/m^3 and P_{amb} = 50 MPa.

X-Ray Radiography Measurements

X-ray radiography measurements were performed at the 7-BM beamline of the Advanced Photon Source at Argonne. Detailed descriptions of the radiography technique as applied to fuel sprays may be found in

previous work [24, 25]. The XRR setup is shown in Figure 3.

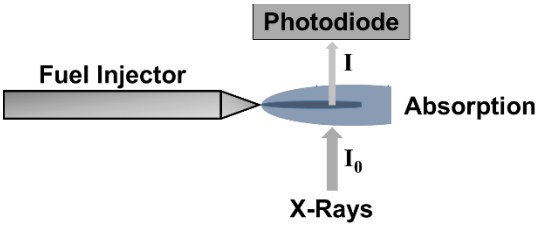

Figure 3. Experimental arrangement for X-Ray Radiography measurements done at Argonne is shown

In brief, a monochromatic beam at 8 KeV energy is passed through a set of curved mirrors which focused the beam to a 5 × 6 µm point. The incoming beam intensity, I_0, was measured using a diamond x-ray beam monitor placed upstream of the pressure chamber. The outgoing beam intensity, I, downstream of the pressure chamber was measured with a PIN diode. As the x-ray beam passed through the fuel spray, photons were absorbed through the process of photoelectric absorption, attenuating the beam by an amount related to the amount of fuel in the beam path. From the change in beam intensity, the projected density of the fuel can be determined with the Beer-Lambert law,

$$\frac{I}{I_o} = e^{-\mu_M \int \rho dz} \tag{3}$$

where μ_M is the fuel absorption constant [area/mass] and $\int \rho dz$ is the projected density in the line of sight [mass/area]. Between 16 and 32 spray events were averaged at each measurement point, and the x-ray beam was raster scanned in both the axial and transverse coordinates to create an ensemble-averaged map of the line-of-sight path length of fuel. Figure 4 provides an example of the 2-D interpolated projected density with the exact measurement points overlaid.

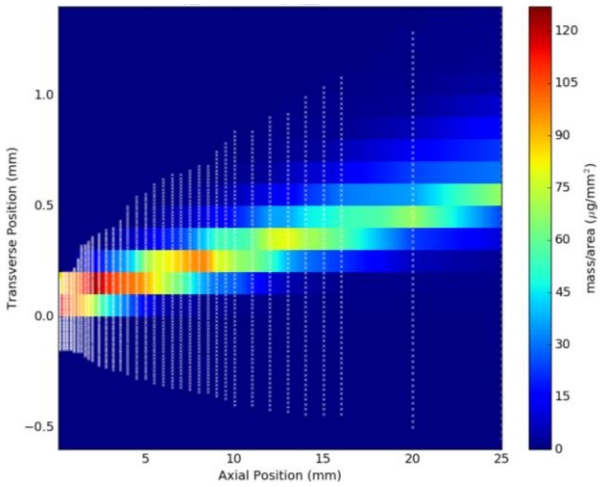

Figure 4. An example 2-D projected density map is shown for Spray D. Experimental conditions: P_{amb} = 1.2 kg/m^3 and P_{amb} = 50 MPa.

From the DBI and radiography experimental results, transverse distributions of optical thickness and projected density can be produced. For this paper, transverse distributions at 10, 16, and 20 mm axial locations for the Spray D 1.2 kg/m^3 ambient density and 50 MPa injection pressure condition are analyzed. To quantify the SMD, several data processing steps were taken. These data processing steps will be the focus of the paper. Before elaborating on the data processing done to extract the SMD, a brief derivation of the theory for the ratio technique is presented here.

Scattering-Absorption Measurement Ratio Technique

Previous work by Magnotti and Genzale have detailed the theory underpinning the relationship between the scattering-absorption measurement ratio and the SMD of the droplet size distribution within the probed measurement volume [13]. Important details of the theory are reproduced here. Using Equation (2), the path-integrated optical thickness measurement can be related to *LVF* and number-weighted means of spray parameters within the probed measurement volume. For isothermal non-vaporizing sprays, the x-ray absorption measurement of projected density can be recast as a measurement of *LVF*. Thus, for overlapping x-ray radiography and diffuse back illumination measurement volumes, the measurement ratio is proportional to SMD, as shown in Equation (4):

$$\frac{LVF}{\tau} \alpha \frac{\overline{\frac{\pi d^3}{6}}}{\overline{C_{ext}}} \alpha \frac{\overline{d^3}}{\overline{d^2}} \alpha SMD \tag{4}$$

To relate the measurement ratio to the *SMD* of the droplet size distribution, the extinction cross-section, C_{ext}, must be determined. Using the publicly available program MiePlot [26], $\overline{C_{ext}}$ is determined for a given SMD, assumed droplet size distribution function, incident light wavelength, measurement collection angle (220 mrad), and liquid index of refraction (1.421 for n-dodecane). As previously shown in [13], the choice of drop size distribution for these calculations does not strongly affect the relationship between the measurement ratio and SMD, and a monodisperse droplet size distribution is assumed for simplicity. An input light wavelength of 633 nm is employed for the calculations, which is selected to be representative of the visible wavelength range of the white LED. We find negligible impact of illumination wavelength choice on our calculations for wavelengths in the visible regime. The measurement ratio is then related to the *SMD* by normalizing the calculated $\overline{C_{ext}}$ by the number-weighted mean droplet volume $\overline{\pi d^3/6}$. Assuming solutions in the Mie-scattering regime, where droplets are larger than the incident wavelength of light, the calculated ratio is used as a look-up table to relate the measurement ratio with SMD.

Joint Processing of Scattering-Absorption Extinction Measurements

Comparing experimental data from two experimental facilities requires careful consideration. One important consideration was that the Spray D injector was oriented in the same manner between both experimental facilities. The injector at ANL was mounted horizontally with the fuel inlet oriented vertically upwards. This position is referred to as the 0° orientation, consistent with the injector orientation nomenclature adopted by the ECN [17]. Unfortunately, due to some experimental limitations, Georgia Tech could not perfectly match ANL's injector orientation, yielding an approximately 10° difference in the relative viewing angles of the spray. To assess the effect of relative errors in measurement viewing angle on the resulting SMD quantified in the joint measurements, the optical thickness/projected density measurement ratio processing was conducted using the DBI data from two different injector orientations, 180° apart. The DBI data is labeled as 0° or 180° to indicate these two different viewing angles and the conclusion regarding the importance of precisely matching the injector orientation will be elaborated upon when discussing the SMD results.

It is also important to ensure that both sets of experimental data are spatially aligned. For example, as shown in Figure 5, the x-ray radiography and DBI measurements utilize different transverse coordinate systems and are co-aligned by centering the full-width half maximum (FWHM) of each distribution about 0 mm. This processing step ensures that the spray centerline is consistently defined at y = 0 mm.

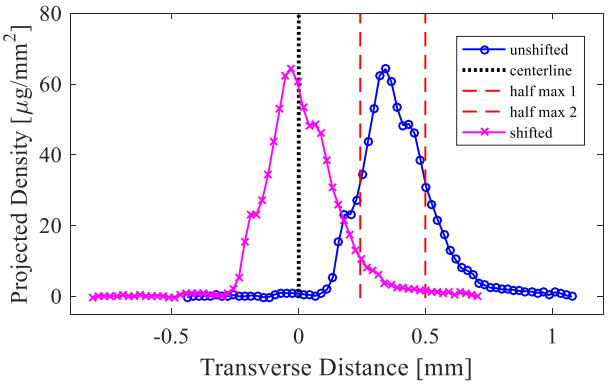

Figure 5. Transverse projected density distribution obtained from x-ray radiography measurements, at a location of 16mm from the nozzle exit. The data has been shifted by centering the FWHM of the distribution at 0 mm.

After both sets of data are co-aligned, it is necessary to resample the data so that the joint measurement analysis is conducted for equivalent measurement volumes. To do this, a binning process was established using the spatial resolution of the DBI measurements (77.7 μm), see figure 6. As discussed later, the projected density data, which features a higher spatial measurement resolution, is ultimately average within the bin centered around the optical thickness measurements.

In addition to binning the data, another important processing step is to identify regions where the optical thickness/projected density measurement ratio can be accurately interpreted. As mentioned before, the measurement ratio can only be taken where the optical thickness is less than 2.0 to ensure that the signal is dominated by single scattering events [22, 23]. In addition to this requirement, the projected density values must be higher than the measurement noise floor (NF = 0.9 μg/mm^2) to ensure that the reported values are meaningful data points. Figure 6 illustrates the binning process and shows the transverse locations where a ratio can be taken ($t \leq 2$ and projected density > NF, green shaded areas) for the 16-mm axial location 0° DBI data.

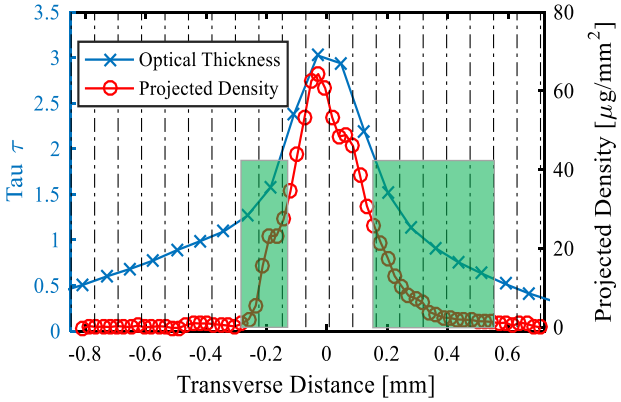

Figure 6. Optical thickness and projected density transverse distributions 16 mm from the injector nozzle, 0° viewing angle. The green shaded boxes show the locations where the measurement ratio can be accurately interpreted (t ≤ 2 and projected density > NF).

Because the measurements inherently contain noise fluctuations, curve fits were executed to extract a smooth distribution curve for each measurement prior to resampling the projected density measurements and executing the measurement ratio. The curve fits were used to quantify the average projected density in each bin. One difficulty in curve fitting the data was that a single functional form could not be applied to all the axial locations. This was because some axial locations had particular features that could not be easily curve fit, such as the "shoulder" seen in the projected density data on the left hand side of the spray (Figure 6). In order to capture these features of the spray, which are repeatable and not likely artifacts of noise, each axial location was individually curve fit, using the *fit* function in MATLAB. All of the employed curve fits had an R^2 value greater than 0.98, indicating good representation of the trends and values of the data points. For these reasons, a customized curve fit was employed for the transverse distribution at each axial location. Figures 7(a) and (b) show the curve fits for the left and right half of the projected density distributions at the 10, 16 and 20-mm axial locations.

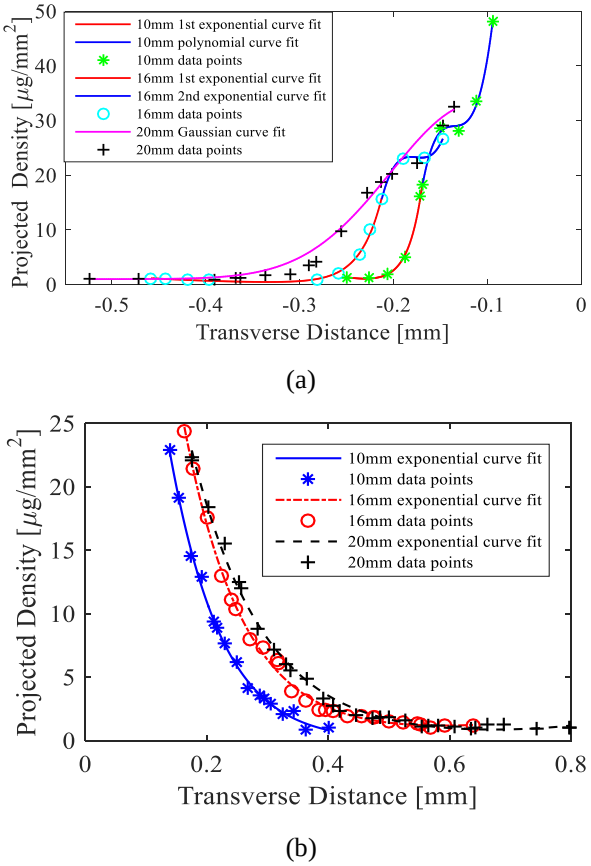

Figure 7. Projected density measurements and their respective curve fits shown for three axial locations (10 mm, 16 mm, and 20 mm) for the left half (a) and right half (b) of the spray.

Figure 7(a) shows the curve fits for the left half of the spray. For the 10 and 16-mm axial locations, two separate curve fits are used to capture the complex shape of the data, namely the "shoulder" in the projected density data. The data is broken up into two segments surrounding the "shoulder." The first segment of data points was fit with an exponential function of the form,

$$f(x) = Ae^{Bx} + Ce^{Dx} \quad (5)$$

where A, B, C, and D are unique fitting coefficients. For the 10mm axial location, the second segment of data points was fit with a three term polynomial function of the form,

$$f(x) = Fx^3 + Gx^2 + Hx + I \quad (6)$$

where F, G, H, and I are unique fitting coefficients. For the 16-mm axial location, the second segment of data points was fit with an exponential function of the form,

$$f(x) = Je^{Kx} + Le^{Mx} \quad (7)$$

Where J, K, L, and M are unique fitting coefficients. The 20-mm location was curve fit using a single Gaussian function, of the form,

$$f(x) = Ne^{-(\frac{x-P}{Q})^2} \quad (8)$$

Where N, P, and Q are unique fitting coefficients.

The left half of the spray for the projected density values tended to show more asymmetries than the right half for this low ambient density and low injection pressure case (see [12] for more details regarding spray asymmetries for these experiments). Figure 7b shows the data points and curve fits for the right half of the spray. For all three axial locations, an exponential curve fit of the form of equation 5 was used for the right half of the spray, which accurately represented the data points.

Once curve fitting the data points was completed, the average projected density in each bin was calculated using the equations found from curve fitting the data (equations 5-8). With the projected density data now resampled and overlaid with the optical thickness measurement points, the measurement ratio is conducted to quantify SMD.

As previously discussed, by taking the ratio of the x-ray absorption and visible-light scattering, it is possible to extract the mean droplet size within the overlapping measurement volume [13]. As shown in Equation 4, this ratio is proportional to the SMD. Figure 7 shows the resulting SMDs quantified for all three axial locations extracted from the joint absorption-scattering measurement. For each axial location, the quantified SMD distribution is shown for two DBI data orientations(0° and 180°).

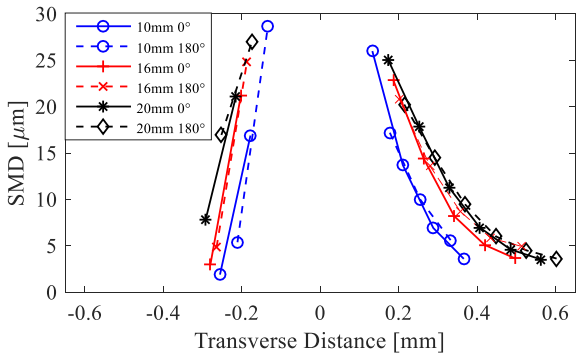

Figure 8. Sauter Mean Diameter as a function of the transverse distance at three axial locations (10 mm, 16 mm, and 20 mm) with the DBI data oriented at 0° and 180°.

Comparison of the SMDs quantified using 0° and 180° orientations of the DBI data enables assessment of the sensitivity of the SMD measurement to relative differences in facility-to-facility injector orientation. For the 10, 16, 20-mm axial locations, SMD distribution shapes on both the left and right half of the spray show very good agreement when the DBI data is oriented at 0° or 180°. This indicates that the relative injector orientation of the DBI and radiography measurements does not cause substantial error in quantifying the SMD distribution at these conditions. However, the data does indicate that there are asymmetries in the spray. As seen in Figure 8, The SMD measurements for the right half of the spray show a more gradual decrease in droplet size with increasing distance from the spray centerline than for the left half of the spray. However, this asymmetry is well reproduced regardless of the DBI data orientation. Thus, while the relative orientation of the DBI data does not appear to strongly affect the quantified SMD distribution, the asymmetry of that distribution is likely to be strongly affected by the orientation of the x-ray radiography measurement.

These measurements also indicate that a dense region of larger sized droplets exist closer to the spray centerline, with smaller sized droplets along the spray periphery. The right half of the spray also shows that the 16-mm and 20-mm axial locations have droplets similar in size. This suggests that a quasi-stable droplet size has been reached at these downstream locations.

The asymmetry observed in the spray SMD distributions indicate that the assumption of a symmetric spray is not always valid, especially at this low backpressure conditions (1 bar). Figure 6 shows that asymmetries are evident in both the DBI and radiography measurement results, particularly evident in the “shoulder” seen in the left side of the projected density data. It is believed that this spray feature, and possibly the source of the observed spray morphology asymmetries, may stem from a machining groove that is present along the interior of the Spray D #209133 orifice [12].

Summary

In this work, we have presented a new scattering-absorption extinction measurement technique, leveraging joint measurements at Georgia Tech and Argonne National Laboratory, to quantify the SMD distribution in ECN Spray D. Quantifying transverse SMD distributions from the joint scattering-absorption measurements involved several data processing steps. These steps included: co-aligning the optical thickness and projected density measurements by centering the

FWHM of the transverse distributions, binning the projected density data in order to compare consistent measurement volumes between the DBI and radiography experiments, identifying the regions where each of the measurements could be accurately interpretted, curve fitting the data, finding an average projected density in measurement volume using this curve fit, taking a ratio of the projected density and optical thickness values, and finally applying Mie-scatter calculations to quantify the SMD.

Several sources of uncertainty in the quantified SMD were identified and addressed in this work. Firstly, one source of experimental uncertainty is due to potential uncertainty in relative positioning between the two measurements. This source of uncertainty was reduced by centering the FWHM of each of the transverse distributions. To minimize the source of uncertainty due to inconsistent measurement volumes, a binning process was established to ensure that corresponding measurement volumes were being analyzed. Finally, the influence of relative injector orientation between the two experimental facilities was analyzed. Comparison of the quantified SMD using DBI measurements at 0° and 180° orientations revealed similar distributions. This indicates that the relative injector orientation between the two facilities may not have a large effect on the quantified SMD values. However, absolute asymmetries in the quantified SMD distribution were observed, indicating that the injector orientation or viewing angle adopted in the x-ray radiography measurements will affect the resulting SMD distribution.

Overall, this new measurement technique provides a rapid methodology to quantify 2-D droplet sizing measurements along the periphery of optically thick sprays using a relatively easy to implement experimental technique. Further application of this measurement technique to a variety of experimental conditions will be helpful in learning more about the spray atomization process as well as for validating spray breakup models.

Future Work

In the future, this technique will be applied to x-ray radiography and diffuse back illumination measurements conducted under other experimental conditions, including higher ambient densities and injection pressures. Evaluating transverse SMD distributions over a broad range of conditions will provide insight into the sensitivity of SMD to changes in injection and ambient conditions. This information is critical to assessing and formulating predictive spray breakup theories and computational models that can capture the experimentally observed trends.

Acknowledgements

This material is based upon work supported by the Department of Energy, Office of Energy Efficiency and Renewable Energy (EERE) and the Department of Defense, Tank and Automotive Research, Development, and Engineering Center (TARDEC), under Award Number DE-EE0007333.

Nomenclature

USAXS	ultra-small angle x-ray scattering
SMD	Sauter mean diameter
ECN	Engine Combustion Network
DBI	diffuse back illumination
τ	optical thickness
LVF	Liquid volume fraction

References

1. Lefebvre A. H., “Atomization and Sprays,” (New York, Taylor and Francis, 1989).

2. Wang, T.C., Han, J.S., Xie, X.B., et. al., “Parametric characterization of high-pressure diesel fuel injection systems,” J. Eng. Gas Turbine Power, 125:412-426, 2003.

3. Peters N., and Weber J., “The Effects of Spray Formation and Evaporation on Mixing, Auto-ignition and Combustion in Diesel Engines,” presented at THIESEL, Valencia, Spain, 2006.

4. Som, S., & Aggarwal, S. K. (2010). Effects of primary breakup modeling on spray and combustion characteristics of compression ignition engines. Combustion and Flame, 157(6), 1179-1193. DOI: 10.1016/j.combustflame.2010.02.018

5. Soare, V., PhD Thesis, Universidad Politecnica da Valencia, 2007

6. Margot et al., SAE Technical Paper 2008-01-0962, 2008.

7. Behrendt, T. et al., Atomization and Sprays, 2006.

8. Kastengren, A. L., Tilocco, F., Duke, D. J., Powell, C., Zhang, X., & Moon, S. (2014). Time-Resolved X-Ray Radiography of Sprays from Engine Combustion Network Spray A Diesel Injectors. Atomization and Sprays, 24(3), 251–272.

9. Kastengren, A., & Powell, C. F. (2014). “Synchrotron X-ray techniques for fluid dynamics.” Experiments in

Fluids, 55(3), 1686. http://doi.org/10.1007/s00348-014-1686-8

10. Kastengren, A.L., Powell, C.F., Arms, D., Dufresne, E.M., Gibson, H. and Wang, J. “The 7BM beamline at the APS: a facility for time-resolved fluid dynamics measurements.” J. Synch. Rad. 19(4):654-657, doi: 10.1107/S0909049512016883.

11. Magnotti, G. M. and Genzale, C. L., 2016. “Characterization of Diesel Spray Breakup Models Using Visible and X-Ray Extinction Measurements” *ILASS-Americas 28th Annual Conference on Liquid Atomization and Spray Systems*, 2016.

12. Magnotti, G. M., Matusik, K.E., Duke, D.J., Knox, B. W., Martinez, G. L., Powell, C. F., Kastengren, A. L., and Genzale, C. L., 2016. “Modeling the Influence of Nozzle-Generated Turbulence on Diesel Sprays” *ILASS-Americas 29th Annual Conference on Liquid Atomization and Spray Systems*, 2017. (submitted)

13. Magnotti, G. M. and Genzale, C. L., 2016. “Detailed Assessment of Diesel Spray Atomization Models Using Visible and X-Ray Extinction Measurements” *International Journal of Multiphase Flows*. (submitted)

14. Magnotti, G.M. and Genzale, C.L., SAE Technical Paper 2017-01-0829, 2017

15. Knox, B. W. “End of Injection Effects on Diesel Spray Combustion” PhD Thesis, Georgia Institute of Technology, 2016.

16. Meijer, Maarten, Bart Somers, Jaclyn Johnson, Jeffrey Naber, Seong-Young Lee, Louis Marie Malbec, Gilles Bruneaux et al. "Engine Combustion Network (ECN): Characterization and comparison of boundary conditions for different combustion vessels." *Atomization and Sprays* 22, no. 9 (2012). DOI: 10.1615/AtomizSpr.2012006083.

17. Engine Combustion Network, “Engine Combustion Network: Injector Spray D Nozzle Geometry,” https://ecn.sandia.gov, accessed March 2017.

18. Matusik, K.E., Duke, D.J. A.B. Swantek, C.F. Powell, and A.L. Kastengren. “High resolution x-ray tomography of injection nozzles.” *ILASS-Americas 28th Annual Conference on Liquid Atomization and Spray Systems*, 2016.

19. Kastengren, A.L., Powell, C.F., Riedel T., Cheong, S.-K., Im, K.-S., Liu, X. Wang, Y.J., and Wang, J. “Nozzle geometry and injection duration effects on diesel sprays measured by x-ray radiography”. J. Fluid. Eng. 130:0413-01-12, doi: 10.1115/1.2903516.

20. Westlye, F.R., Penney, K., Skeen, S., Manin, J., Pickett, L. and Ivarsson, A., 2016. “Experimental Setup for High Temporal Diffuse Back-Illumination Measurements.” *Applied Optics* (submitted)

21. Bohren, C. F. and Huffman, D. R., *Absorption and Scattering of Light by Small Particles*, Wiley, New York, 1983.

22. Berrocal, E. “Multiple Scattering of Light in Optical Diagnostics of Dense Sprays and other Complex Turbid Media” PhD Thesis, Cranfield University, 2006.

23. Berrocal, E. Churmakov, D. Y., Romanov, V. P. Jermy, M. C. and Meglinski, I. V., 2005. "Crossed source–detector geometry for a novel spray diagnostic: Monte Carlo simulation and analytical results," *Applied Optics* 44, 2519-2529.

24. Kastengren, A.L., Powell, C.F., Riedel T., Cheong, S.-K., Im, K.-S., Liu, X. Wang, Y.J., and Wang, J. “Nozzle geometry and injection duration effects on diesel sprays measured by x-ray radiography”. J. Fluid. Eng. 130:0413-01-12, doi: 10.1115/1.2903516.

25. Kastengren, A.L., Powell, C.F., Arms, D., Dufresne, E.M., Gibson, H. and Wang, J. “The 7BM beamline at the APS: a facility for time-resolved fluid dynamics measurements.” J. Synch. Rad. 19(4):654-657, doi: 10.1107/S0909049512016883.

26. http://www.philiplaven.com/mieplot.htm, accessed March 2017.